HNPS Advances in Nuclear Physics

Vol 5 (1994)

HNPS1994

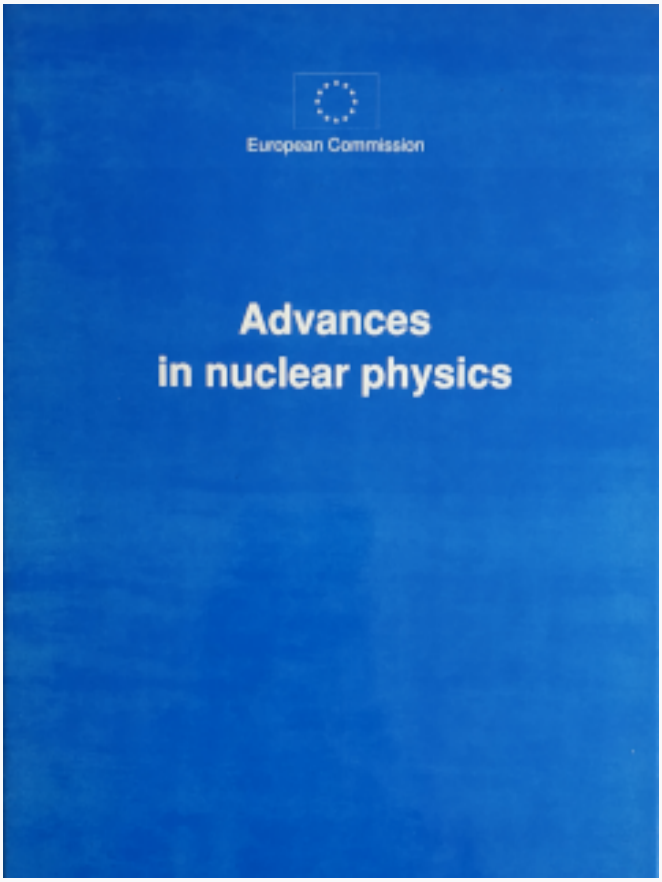

Power Deposition Profile and Suprathermal Energy Spectra From Modulated ECRH

H. J. Hartfuss, V. Erckmann, A. Kechriniotis, H. Maassberg, M. Romé, and the W7-AS-Team

doi: 10.12681/hnps.2908

POWER DEPOSITION PROFILE AND SUPRATHERMAL ENERGY SPECTRA FROM MODULATED ECRH

H.J. Hartfuss, V. Erckmann, A. Kechriniotis*, H. Maassberg, M. Romé and W7-AS-Team
Max-Planck-Institut für Plasmaphysik, 85748 Garching, Germany
*University of Patras, Greece

Introduction

Heat wave studies from ECRH power modulation experiments have been conducted in the W7-AS stellarator under a variety of plasma conditions and heating scenarios [1, 2]. To generate the heat wave, the electron temperature is being locally varied by modulating the ECR heating power, introducing a small temperature perturbation (< 10%) whose radial propagation away from the power deposition zone is studied by means of a 24 channel ECE heterodyne radiometer of the type described earlier [3], monitoring the spatial and temporal evolution of the electron temperature. In all the experiments described second harmonic X-mode emission is measured from the low field side of W7-AS in a toroidal plane with 1/R B-field dependence. The analysis of the transient power balance in ECRH modulation experiments gives additional information on the physics of the electron heat transport $\tilde{q}_e$ in combination with the stationary analysis. No dependence of the electron thermal diffusivity on the electron temperature and the electron temperature gradient could be found [4]. It was found that the incremental diffusivity [5] determined in modulation experiments at W7-AS agrees within the error bars with the heat diffusivity as determined from stationary power balance analysis, and that it scales with plasma parameters like heating power, electron density and rotational transform in the same way as the power balance derived values. This result contrasts with the tokamak findings where usually the incremental diffusivity is clearly higher than the corresponding power balance result, and scalings different to those of the power balance values are observed [6].

In the course of these experiments and parameter studies the modulation frequency, f_{mod}, was varied in the range between 20 Hz and 10 kHz. This paper describes observations made at higher f_{mod} where information on the power deposition profile and on the suprathermal electron energy spectra is obtained. In this higher f_{mod} range, the electron heat transport plays only a minor role.

ECRH power deposition profile

The quantities measured in heat wave experiments are the phase delay and the amplitude decay of the temperature modulation, $\tilde{T}_e$, as a function of distance to the power deposition zone. Besides power switching experiments [7] heat wave propagation offers a tool for deter-

mining the ECRH power deposition profile which is of fundamental interest both for ECRH physics reasons as well as for instance the correct interpretation of heat transport studies. In a 1-D description the amplitude of the temperature modulation decays exponentially with distance, the decay length λ of the temperature perturbation being dependent on the heat diffusivity χ and the ECH power modulation frequency,

$$\lambda = \sqrt{\frac{2\chi}{3\pi f_{mod}}} .$$

With increasing frequency the decay length decreases, at high frequencies it becomes small compared to the extent of the region where heating power is deposited. Measurable temperature modulation then only exists in this region. The behaviour is of course a consequence of the time dependent power balance equation,

$$i\frac{3}{2}n_e 2\pi f_{mod}\tilde{T}_e(r) + \frac{1}{r}\frac{\partial}{\partial r} r\tilde{q}_e + \frac{d}{dT_e}(P_{ei} + P_{rad})\tilde{T}_e = \tilde{P}_{ECRH}(r) .$$

Neglecting the collisional electron-ion coupling, P_{ei}, and the radiative losses, P_{rad}, which are both small in purely ECRH heated plasmas of W7-AS at electron densities below about 4×10^{19} m^{-3}, in the limit of high modulation frequency the term containing the heat flux, $\tilde{q}_e$, becomes also negligible, the temperature modulation profile then approaches the power deposition profile.

Figure 1 gives two examples of modulation amplitude profiles measured at modulation frequencies of 92 Hz and 5000 Hz. While at 92 Hz the heat wave propagation plays a major role, at 5000 Hz the decay length is smaller than 0.5 cm, the modulation amplitude profile therefore approaches the power deposition.

To determine the limiting profile, in the most simple approach, the full width at half maximum (FWHM) of the temperature modulation profiles $\tilde{T}(r)$ which have been fitted by Gaussians are plotted against the modulation frequency (Fig. 2a). The plot gives also the extrapolation of the FWHM to high modulation frequency as obtained by 2nd order Lagrange extrapolation with respect to $1/f_{mod}\rightarrow 0$. The figure shows the results of two modulation frequency scans obtained under constant plasma conditions but heating the plasma with different 70 GHz gyrotrons (GyB and GyD) which have been supplied with beamlines forming Gaussian beams with different width of the beam waist. The resulting power deposition profiles clearly reflect this difference. The FWHM evaluated for the two cases are 5.5 and 3.7 cm respectively. Nevertheless the different beam widths do not affect the stationary temperature profile.

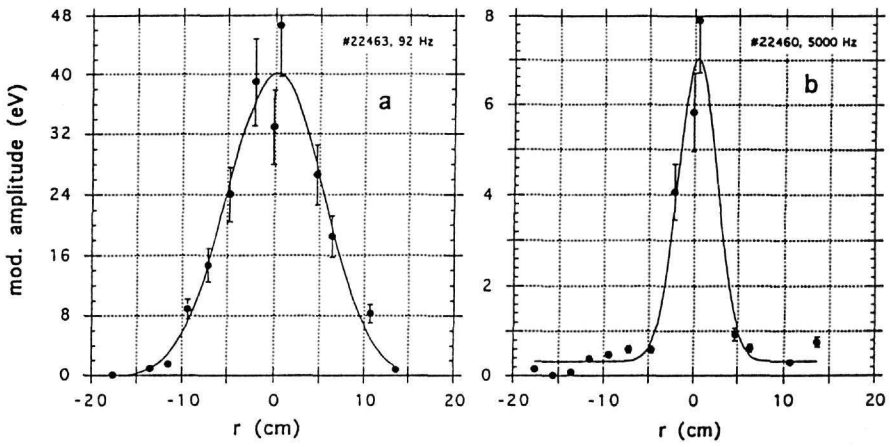

Figure 1: Measured electron temperature modulation amplitudes for two different modulation frequencies 92 Hz (a) and 5000 Hz (b). The data points are fitted by Gauss curves.

In Fig. 2b the extrapolated normalized deposition profile for the narrower launching geometry (GyD) is plotted together with the normalized stationary electron temperature profile demonstrating the good localization of the heating power.

By means of a 3-D Hamiltonian ray-racing code where the absorption and emission coefficients are computed in the weakly relativistic approximation for Maxwellian distribution functions, the ECRH power deposition as well as the quasi-linear diffusion tensor (only the $Q_{\perp\perp}$ element being important) are estimated. For 2nd harmonic X-mode launching, nearly complete single pass absorption is predicted. For fundamental O-mode launching, about 60 – 90 % single pass absorption is obtained for typical conditions and therefore the second pass absorption is taken into account in the calculations.

For the 2nd harmonic X-mode case, about 70 % of the input power is found within the innermost 4 cm (Fig. 3). The width of the deposition profiles as determined by ray tracing and in a more detailed analysis from least squares fitting to the transient power balance as well as from local Lagrange extrapolation of the measured modulation amplitudes at high f_{mod} are identical within the error bars. The much broader background part from this analysis indicates a deposition to the thermal bulk distribution (only this is visible in the ECE measurement) of the order of 20 % . This value is connected with larger error bars due to the extremely low modulation amplitudes involved.

In the W7-AS stellarator no profile resilience is observed. Peaked electron temperature profiles for on-axis heating and broad and flat ones in the off-axis case are observed.

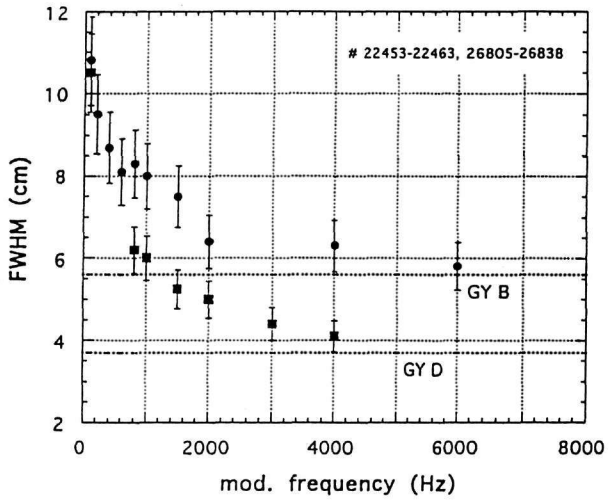

Figure 2a: The full width at half maximum (FWHM) of the Gauss fitted temperature modulation profiles as a function of modulation frequency for two different ECRH beamlines. The limiting values obtained by Lagrange extrapolation are given by the dotted lines labeled Gy B and GyD.

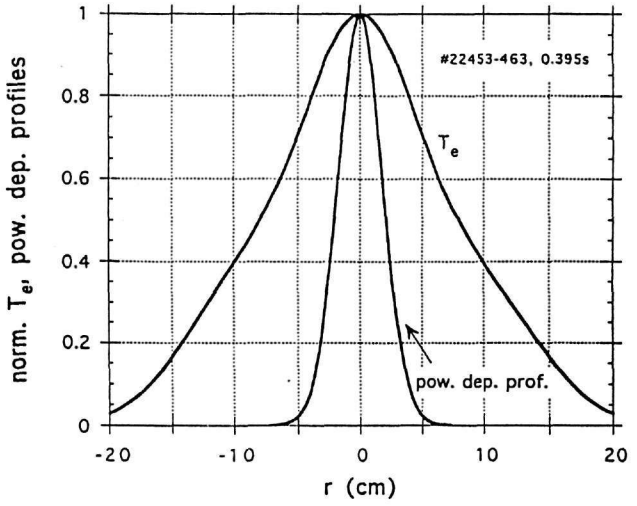

Figure 2b: Normalized electron temperature profile (T_e) in comparison with the normalized power deposition profiles as obtained from an extrapolated modulation frequency scan.

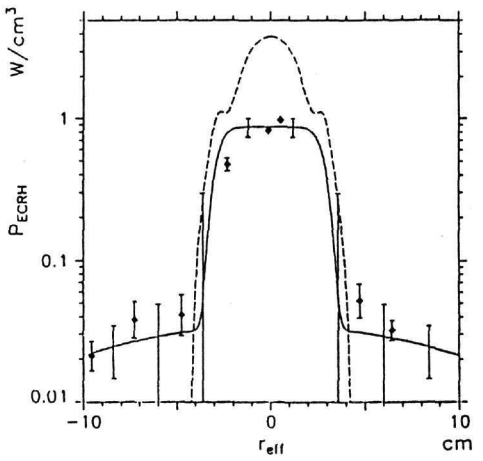

Figure 3: ECRH power deposition profile from transient power balance analysis (solid line) and least squares Lagrange extrapolation (dots) from a modulation frequency scan with special attention to the broad background deposition. For comparison the single path ray-tracing result is included (dashed line).

Figure 4a gives an example for fundamental O-mode heating with off-axis power deposition. Also shown is a Gaussian fit to the Lagrange extrapolated power deposition profile (based on f_{mod} = 2 and 4 kHz), which is in reasonable agreement with the profile from ray-tracing calculations (Fig. 4b). About 55 % of the input power is found compared to 75 % from single pass absorption in the ray-tracing calculation for this case.

The main source of errors in these kind of experiments is the limited signal to noise ratio of the ECE temperature measurement. At high modulation frequencies the temperature modulation amplitude is only of the order of 1 eV in the maximum of the profile. The noise level due to the thermal nature of the ECE clearly exceeds this value [8]. Therefore long stationary phases are necessary to get sufficient signal to noise ratio for the Fourier analysis of the temperature signals. A second source obvious in the on-axis experiments (Fig. 1b) is the limited number of temperature channels within the power deposition zone. The radial spacing of successive channels is not close enough for an accurate determination of the form of the power deposition profile. Therefore just Gaussians are used as a first approximation. For future experiments the W7-AS ECE radiometer has been supplemented by a filterbank which covers the 7 cm surrounding of the plasma centre with 16 additional channels for improved spatial resolution.

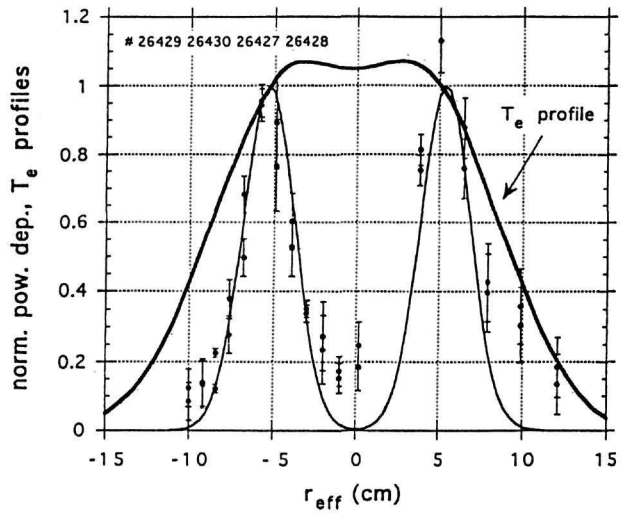

Figure 4a: The normalized electron temperature profile in comparison with the power deposition profile from a modulation frequency scan for off-axis power deposition. Measured data points for 2 and 4 kHz are included which are taken as the basis for the extrapolation.

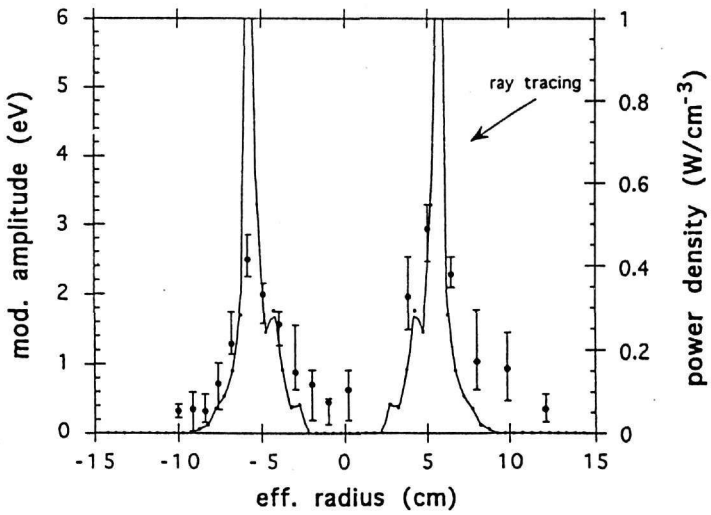

Figure 4b: Modulation amplitudes for 4 kHz modulation frequency in comparison with ray-tracing calculations.

Phase space diffusion effects

During ECRH the electron energy distribution function deviates from a Maxwellian giving rise to down-shifted EC emission resulting in the well known feature at the low frequency end of the ECE spectrum. While the main peak in the spectra is related to thermal emission where reabsorption is essential, the down-shifted peak in the spectral range from 64 to 68 GHz is attributed to a suprathermal tail in the electron distribution (relativistic effect in the resonance condition) with reabsorption being negligible.

If the ECRH is power modulated, the down-shifted emission is modulated too. Figure 5 gives examples of the modulated ECE spectra as measured at ECRH modulation frequencies between 92 and 8000 Hz showing both the thermal and the non-thermal component of the ECE spectrum. Due to the reasons discussed before the width of the thermal spectrum shrinks and the absolute value of the temperature modulation amplitude decays with increasing modulation frequency. Simultaneously the non-thermal feature decays too, but it decays stronger with frequency than the thermal part.

At high modulation frequencies, the deviations of the distribution function from the Maxwellian can lead to significant effects. These kinetic features are estimated using a very simple 1-D Fokker-Planck model with a modulated quasi-linear heating term and the

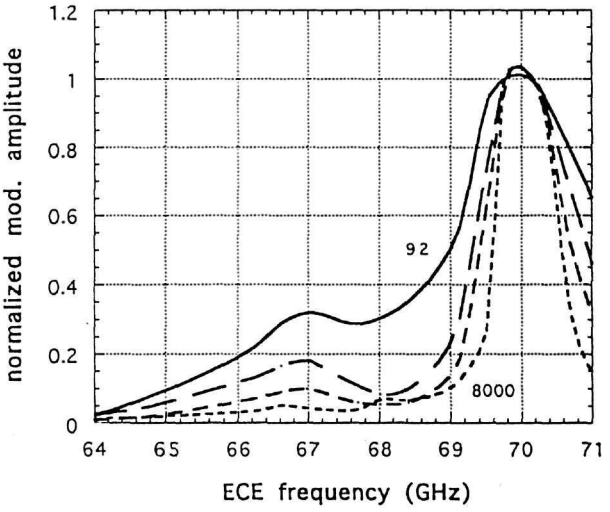

Figure 5: The normalized modulation amplitude as function of ECE frequency given for a sequence of modulation frequencies between 92 and 8000 Hz. The second maximum at the low frequency end of the spectrum corresponds to down-shifted non-thermal emission. It decays stronger with increasing modulation frequency than the thermal emission.

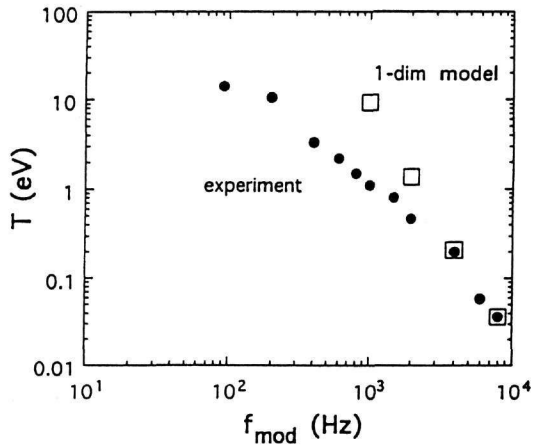

Figure 6: Modulation amplitude of the 67 GHz channel as function of modulation frequency in comparison with 1-D Fokker-Planck calculations. The deviation at low frequencies is due to diffusive transport which is being neglected in the model.

T_e-modulation as the loss term.This temperature modulation (corresponding to the 70 GHz channel in Fig. 5) decays proportional to $(f_{mod})^{-1}$ at $f_{mod} < 10$ kHz if the velocity of the resonant electrons (in the quasi-linear heating term) is typically within the range 1-2 times the thermal one. The estimation of the quasi-linear diffusion tensor (by ray-tracing) gives the same values. At higher modulation frequency or higher resonant velocities, the velocity space diffusion from the quasi-linear heating zone to the thermal bulk results in a much stronger decrease of the modulation amplitude with modulation frequency.

The modulation amplitude in the down-shifted part of the ECE spectrum (s. Fig. 5) being related to the suprathermal tail of the distribution function decays roughly $(f_{mod})^{-2}$ at large f_{mod}. Figure 6 shows the modulation frequency dependence of the "nonthermal" part of the ECE spectrum.

Assuming that the down-shifted emission originates only from the very narrow region with maximum power absorption leads to energies in the range 25 to 50 keV. With reabsorption omitted, the ECE amplitudes are related to the electron energy spectrum suggesting a rather slow decrease with energy (> 10 keV in terms of a bi-Maxwellian modelling). This consequence however is in contradiction to the Fokker-Planck modelling if no "artificial" heating of the high energy tail is introduced.

A less conflicting picture is related to the assumption of a suprathermal electron population much broader than the narrow power deposition zone. Especially for the "standard" configuration of W7-AS at lower rotational transform (0.34), a significant part of the power is ab-

sorbed by ripple trapped electrons within the poloidal plane of ECRH launching . Two effects have to be considered:

i) an increased degradation of the quasi-linear heating efficiency being related to an increased tail formation in the suprathermal distribution and

ii) the radial drift ($v\nabla_B \propto$ to energy) of these ripple trapped suprathermal electrons with mainly collisional detrapping outside of the deposition zone. In this picture, the radial distribution and the energy spectra are strongly linked.

Discussion and Conclusions

The power deposition profiles estimated from ray-tracing calculations are reasonably well confirmed by the analysis of the electron heat wave propagation at high modulation frequencies. Taking into account also the broadened power deposition, the launched power and the absorbed power agree within the error bars.

In specific magnetic configurations in the W7-AS stellarator, the highly focused ECRH leads to very high power densities especially for the electrons being trapped in the local mirror within the launching plane. First Fokker-Planck estimates indicate strong tail formation. Radial grad B drift and collisional detrapping of these suprathermal population may be responsible for the broadening in the "effective" power deposition profile (with respect to the thermal bulk) as well as for the observed "non-thermal" features in the down-shifted ECE.

Power modulation experiments in magnetic configurations with either a local maximum or a stronger minimum of the magnetic induction in the ECRH launching plane are planned in order to investigate the role of trapped particles. In addition, vertical ECE measurements will give information on suprathermal populations. A "bounce-averaged" Fokker-Planck code for the relevant W7-AS configurations being under development is essential for a quantitative description of the physics involved.

References

[1] L. Giannone et al., Nucl. Fus. 32, 1985 (1992)

[2] H.J. Hartfuss et al., Nucl. Fus. 26, 678 (1986)

[3] H.J. Hartfuss, M. Tutter, Rev. Sci. Instr. 56, 1703 (1985)

[4] H.J. Hartfuss et al., Plasma Phys. Control. Fusion 36, B17 (1994)

[5] N.J. Lopes Cardozo et al., Plasma Phys. Control. Fusion 32, 983 (1990)

[6] N.J. Lopes Cardoso et al., Nucl. Fus. 30, 521 (1990)

[7] V. Erckmann and U. Gasparino, Plasma Phys. Control. Fusion 36, 1869 (1994)

[8] S. Sattler, H.J. Hartfuss, Plasma Phys. Control. Fusion 35, 1285 (1993)